

A. ȘTEFAN¹, D.-L. CHICET^{2*}, B. ISTRATE¹, C. MUNTEANU^{1,3}

COLD SPRAY COATINGS MORPHOLOGY

In the Cold Spraying technology, the coatings are produced as a result of the supersonic acceleration of the particles in a gas jet, at temperatures below the melting/phase transformation point of the sprayed material. In this paper, the morphology of a Ni/CrC cold spray coating is studied, based on the identification of the particle's characteristic at various magnifications, both on cross-section and on the surface of the samples. The layer appearance is continuous, uniform and sinuous, no adhesion defects were observed at the substrate-coating interface, and the plastic deformation of the steel was highlighted. The elemental chemical analysis on the sample cross-section, together with the distribution map shows that the carbide particles have retained their sphericity to a large extent, being uniformly embedded in the Ni matrix, as a result of the plastic deformation. This allows a higher thickness of the cold spray coatings comparatively to the ones obtained with the other thermal spray methods that imply high temperatures of the gas jet and layered microstructures.

Keyword: Cold spray coatings; microstructure; morphology

1. Introduction

Cold spraying (CS) is a relatively recent thermal spraying technique that belongs to a broader range of thermal spraying processes, with differently named approaches including: Cold Gas Dynamic Spray, Kinetic Spray, High Velocity Particle Consolidation (HVPC), High Velocity Powder Deposition, and Supersonic Particle/Powder Deposition (SPD) [1]. In this process, powder particles are accelerated by supersonic gas jets to a temperature that is always below the melting point of the material, resulting in a solid particle coating and thus eliminating the process of powder melting and solidifying as in conventional thermal spraying [2,3].

The basic principle of cold spraying is quite simple. A very high-velocity gas jet (300-1200 m/s) generated using a DeLaval nozzle or similar convergent/divergent nozzle is used to accelerate the powder particles (1-1200 m/s) 50 μm is sprayed onto the substrate about 25 mm from the nozzle outlet, where it hits to form a coating [4]. The kinetic energy of the particles, instead of the temperature rise, contributes to the formation of splashes, due to the plastic deformation of the particles on impact [5]. Thus are avoided or minimized many of the harmful disadvantages of conventional thermal spraying methods: oxidation, evaporation, melting, crystallization, residual stress, or gassing [6]. In this

process, powder particles are accelerated by a supersonic gas jet to a temperature always below the material's melting point, forming a coating of completely solid particles, so that the powder does not go through the melting and solidification process of traditional thermal spraying processes [7,8]

Interest in CS has grown relatively quickly over the last two decades, as evidenced by the number of publications per year, as shown in the graph in Fig. 1. Academic publications on

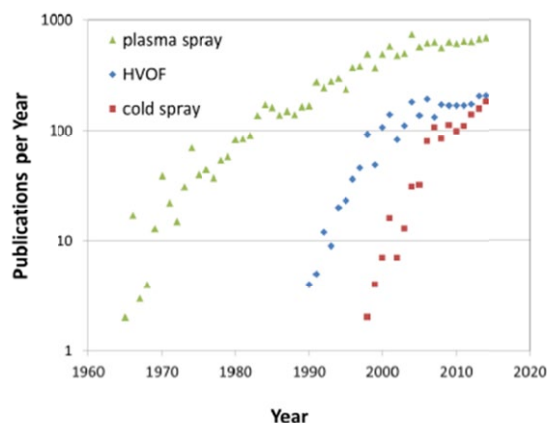


Fig. 1. The trend in research interest in cold spraying, as measured by the number of publications per year, compared to plasma spraying and high velocity oxy-fuel spraying [5]

¹ GHEORGHE ASACHI TECHNICAL UNIVERSITY OF IASI, DEPARTMENT OF MECHANICAL ENGINEERING, BLVD. MANGERON, NO. 61, 700050, IASI, ROMANIA

² GHEORGHE ASACHI TECHNICAL UNIVERSITY OF IASI, DEPARTMENT OF MATERIALS SCIENCE AND ENGINEERING, BLVD. MANGERON, NO. 41, 700050, IASI, ROMANIA

³ TECHNICAL SCIENCES ACADEMY OF ROMANIA, 26 DACIA BLVD, BUCHAREST, 030167, ROMANIA

* Corresponding author: daniela-lucia.chicet@academic.tuiasi.ro



CS include several books and review articles covering various aspects of the process and its applications [9,10]. The subject is broad and covers various research areas from fluid dynamics to solid mechanics.

Even from a materials perspective, there are various aspects related to material properties and relevant physical phenomena that deserve separate analyses: different particle size ranges of copper powders ($-25 + 5 \mu\text{m}$) were sprayed with nitrogen gas and dense coatings were obtained using a broad range of gas inlet pressure and temperature [11]; different problems regarding the flow in the nozzle and the jet outflow in the case of a supersonic nozzle with a rectangular exit section and a Mach number between 2 and 3.5 were studied [12]; the prediction of the necessary requirements for metallic materials cold spraying and the establishment of the optimum spray conditions for bonding at maximum acceleration [13,14]; the importance of surface activation with abrasive particles anterior the coating process [15].

The major advantage over thermal spraying techniques is the low temperatures involved, which minimizes any potential phase change and keeps the particles in their solid unchanged state. The difference between the cold spray process and other thermal spray processes is illustrated in Fig. 2.

In the thermal spraying process, a coating is formed by melting the coating material and then rapidly cooling the molten droplets. Therefore, in general, thermal spray coatings have microstructures with varying degrees of porosity, oxides and other inclusions, and low corrosion resistance characteristics [17]. However, the CS process has the advantage of low heat input metal deposition, local deposition on a limited area and deposi-

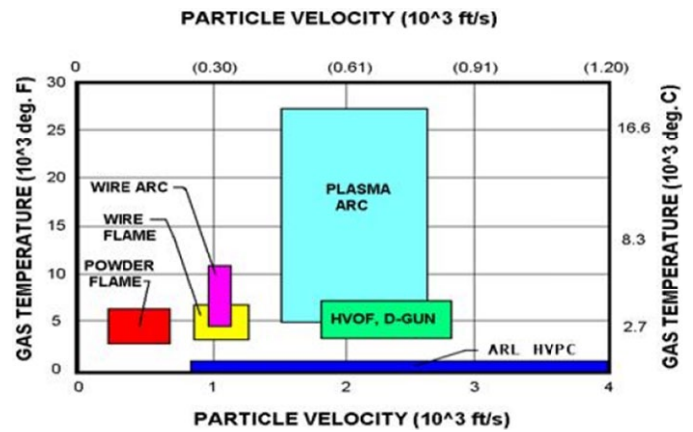


Fig. 2. Comparison of different thermal spraying processes [16]

tion without oxides and other inclusions on any metal surface. Also, due to the compressive stresses, a dense and uniform deposition of any thickness can be achieved, with a microstructure similar to that of the powder material. In addition, excess pulverized raw material can be collected for reuse [2,17].

2. Materials and methods

2.1. Coating process

In this study a substrate of AISI 4340 medium carbon, low nickel-chromium-molybdenum alloyed steel (see TABLE 1), known for its hardness and strength in relatively large cross-

TABLE 1

Chemical composition [wt.%] and equivalent grades of 4340 steel

Equivalent grades	Grade	C	Mn	P	S	Si	Ni	Cr	Mo
ASTM A29	4340	0.38-0.43	0.60-0.80	0.035	0.040	0.15-0.35	1.65-2.00	0.70-0.90	0.20-0.30
EN 10250	36CrNiMo4/1.6511	0.32-0.40	0.50-0.80	0.035	0.035	≤0.40	0.90-1.20	0.90-1.2	0.15-0.30
BS 970	EN24/817M40	0.36-0.44	0.45-0.70	0.035	0.040	0.1-0.40	1.3-1.7	1.00-1.40	0.20-0.35
JIS G4103	SNCM 439/SNCM8	0.36-0.43	0.60-0.90	0.030	0.030	0.15-0.35	1.60-2.00	0.60-1.00	0.15-0.30

TABLE 2

Ni-Cr coating deposition parameters

Parameter	Value
Gas	Nitrogen
Pressure	6.2 MPa (900 psi)
Temperature	675°C
Nozzle type	WC NNZL0060
Nozzle throat size	2 mm
Powder feeder speed	8 rpm
Carrier gas speed	105 slm
Spray distance	25 mm
Spray angle	90°
Spray speed at nozzle level	250mm/s
Spray pitch (nozzle travel)	0.5 mm
Target layer thickness	0.508 mm
Deposited powder	WIP - C1
Deposited powder for intermediate layer	WIP - BC1 și 60°

sections, was used. 4340 alloy steel is generally supplied hardened and tempered in the tensile range of 930-1080 MPa. Pre-hardened and tempered 4340 steels can be further surface hardened by flame or induction hardening and nitriding. Steel 4340 has good shock and impact resistance as well as wear and abrasion resistance in quenched and tempered conditions. The properties of AISI 4340 steel provide good ductility in the annealed state, which allows it to be deformed. ASTM 4340 is often used where other alloy steels do not have the hardenability to provide the required strength, making it a very good choice for highly mechanically loaded parts.

The test samples were realized in a larger study [18] by coating with a mixture of chromium carbide and Ni powder using a Gen-III cold spray plant (VRC Metal Systems, LLC, SD, USA). The parameters used for spraying the mixture are shown in TABLE 2 [19].

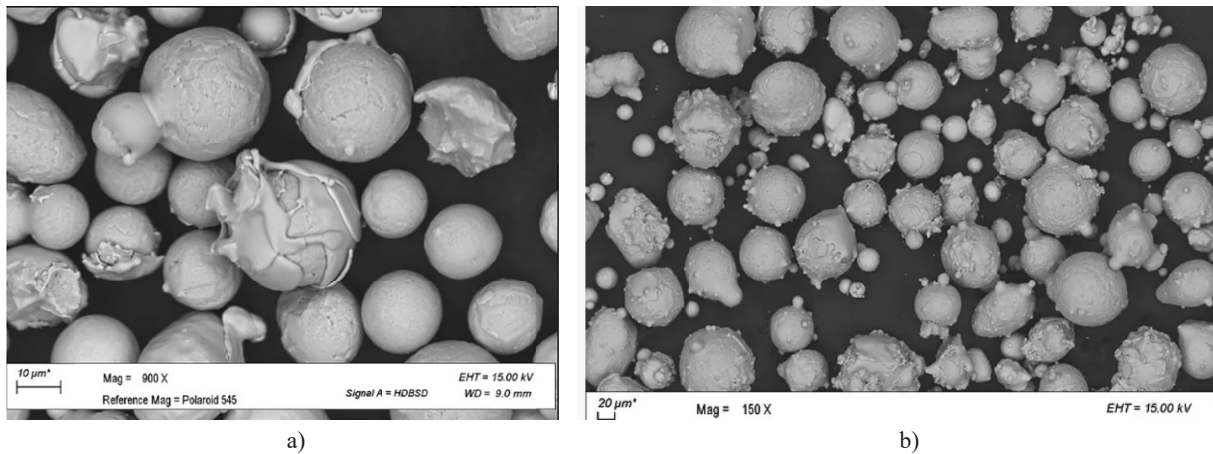


Fig. 3. Appearance of particles forming WIP C1 powder at 150 \times and 900 \times magnification, respectively, WIP BC1 (150 \times)

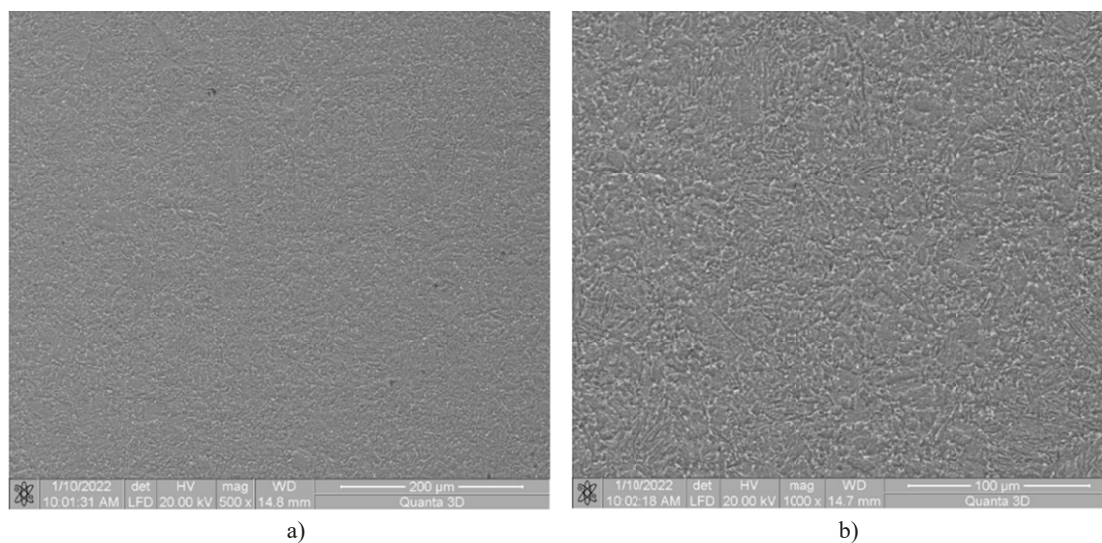


Fig. 4. Images of secondary electrons on AISI 4340 steel substrate cross-section: a) 500 \times , b) 1000 \times

The powder mixture is known commercially as WIP-C1, the appearance of the powder is shown in Fig. 3a. Before the surface was coated with the WIP-C1 powder, a thin intermediate layer of WIP-BC1 powder was applied to the surface (see Fig. 3b) with a nozzle orientation of 60 degrees. This operation was performed for the effect of surface cleaning and increasing the active surface, i.e. the surface roughness, in addition to the formation of a thin layer of bond coat with the role of improving the adhesion of the top coat (WIP-C1).

2.2. Coatings characterisation

For the analysis of the morphology of the coatings, the classical methods of analysis were used: direct observation and optical and electron microscopy, the latter being the most widely used, together with elemental chemical analysis using the EDS method. Two modes were used for electron microscopy image acquisition: Low Vacuum mode, with LFD (Large Field Detector) detector at 20 kV and High Vacuum mode, with ETH detector at 30 kV.

3. Results and discussion

3.1. Morphological analysis

The morphology of the coatings was analyzed both in cross-section (in section), longitudinally (on the surface) and in fracture, with all approaches aimed at providing a complete picture of the structure of the deposited layer.

Microstructural analysis of 4340 steel shows a specific structure of low alloy hypoeutectoid steel with pearlite and low alloy alpha ferrite. Uniformly distributed globular carbides were also identified, as can be seen in Figs. 4a, 4b.

Fig. 5 shows the morphology of WIP BC1 and WIP C1-Ni/CrC coatings by identifying characteristic particles at different magnifications on the surface of one of the samples analyzed. The particle size on the surface ranges from 15-65 microns with a relatively uniform distribution, showing two phases. Compared to other deposition techniques (such as APS) in the TUIASI equipment, flattened particle structures are observed, while splat-like structures due to spray melting are specific to plasma jet spraying [20].

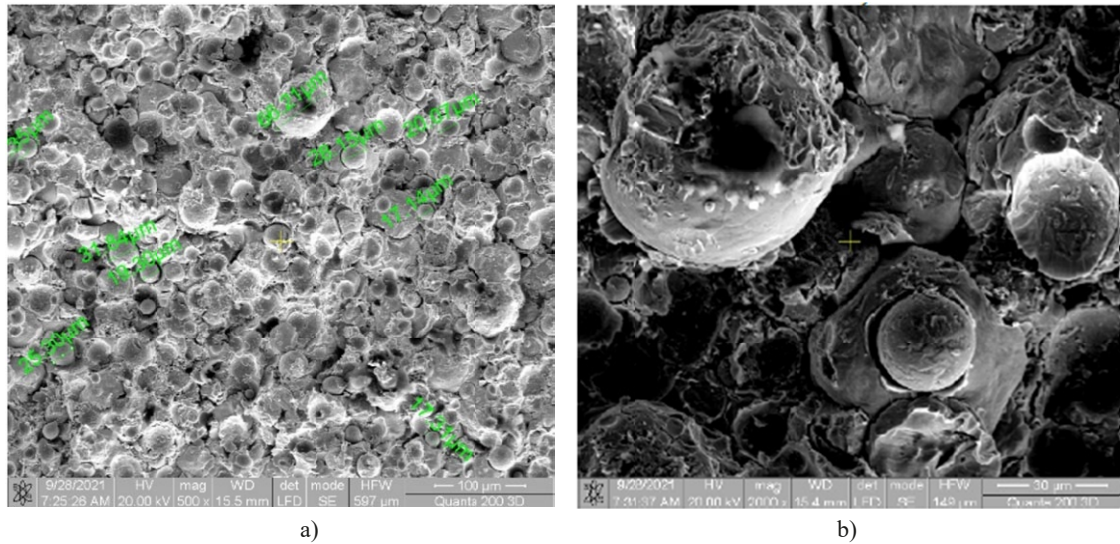


Fig. 5. Images of secondary electrons on the surface of a deposited layer of WIP C1-Ni/CrC: a) 500 \times , b) 2000 \times

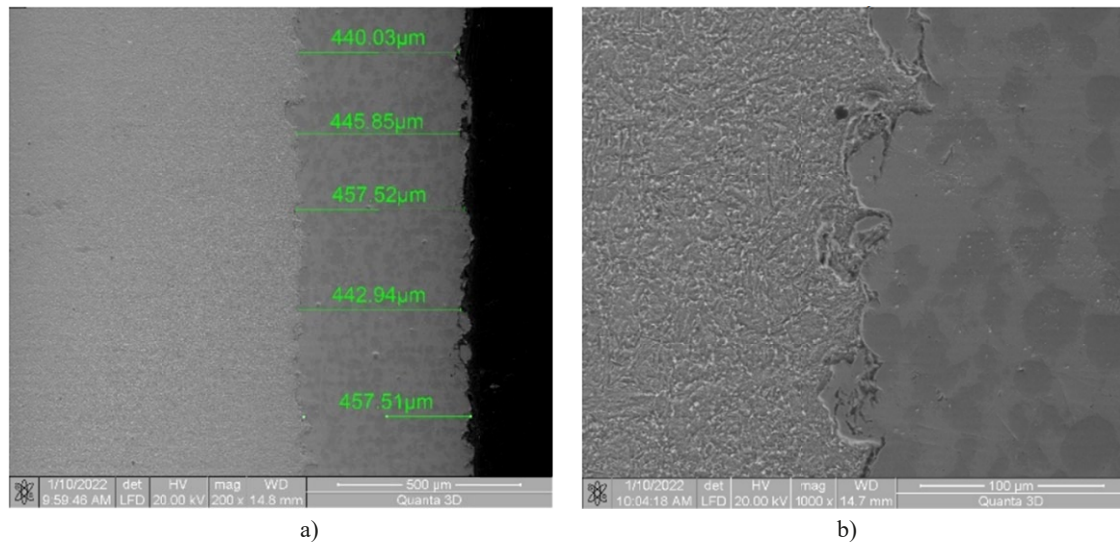


Fig. 6. Cross-sectional aspect of WIP C1-Ni/CrC (20 kV) coating: a) 200 \times , b) 1000 \times

In the cross-sectional analysis shown in Fig. 6, it is observed that the layer has an average thickness of $450 \mu\text{m} \pm 10 \mu\text{m}$, which ensures uniform coverage and a pre-dilution behavior at any point on the surface of the deposited layer.

Figs. 7 and 8 show the morphology of the WIP C1-Ni/CrC deposited layer at different magnification powers analyzed in HV mode at voltages of 30 kV.

Fig. 7 shows that there are no adhesion defects at the coating-deposited layer interface and the appearance is continuous, uniform and sinusoidal, characteristic of these types of coatings. It can also be seen that the 4340 steel substrate has also locally undergone major plastic deformation over a depth of a maximum $20 \mu\text{m}$ at the contact with the deposited layer, as a result of supersonic impact with the sprayed particles during coating.

Fig. 8 shows the cross-sectional appearance of the Cold Spray deposited layer at different magnifications, again showing the very strong interactions between the sprayed particles.

Fig. 9 shows secondary electron images taken in several areas on the surface of the samples studied. The irregular appearance specific to Cold Spray coatings is observed, due to the successive deposition of sputtered particles, which either retained their shape due to their high specific hardness (case of CrC particles) or deformed very much forming an embedding layer of the previous ones (case of Ni-based powders). With increasing magnification power, the plastically deformed matrix and the undeformed spheres are more and more clearly observed, which together generate the roughness of the coating.

A third way of morphological analysis addressed was also that of the appearance of the fracture resulting after the breakage [18] of the samples following the fatigue tests, the images of secondary electrons at different magnification powers are shown in Fig. 10. The uniform distribution of hard CrC particles throughout the matrix is observed, as well as the granular and intergranular breakage of the Ni matrix, concomitant with the detachment (loss of adhesion) of the hard formations.

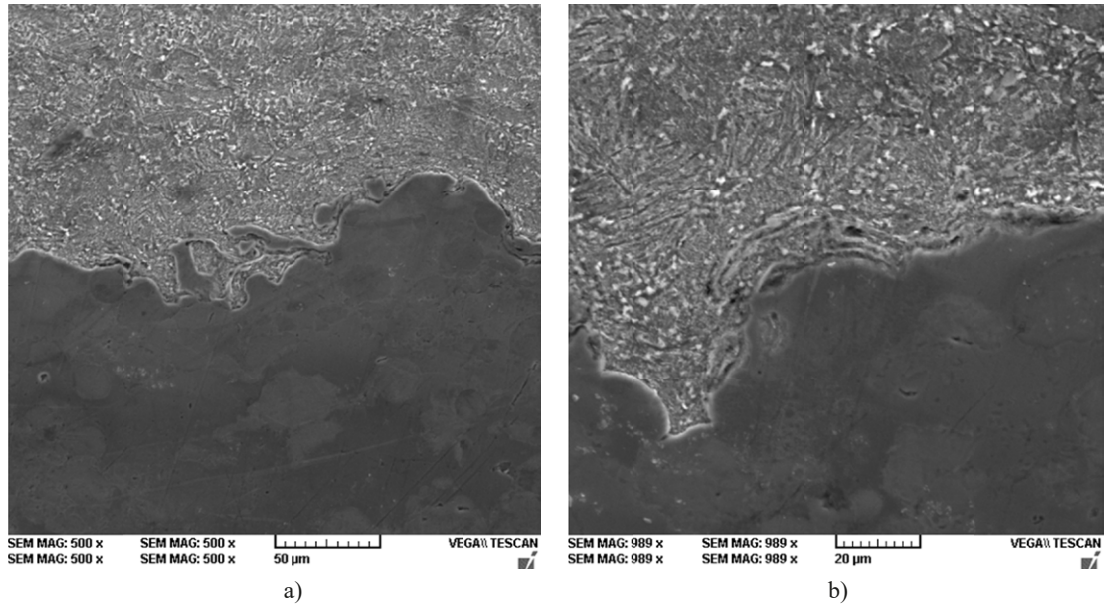


Fig. 7. Cross-sectional images of secondary electrons at the coating (top) – substrate (bottom) interface: a) 500×, b) 2000×

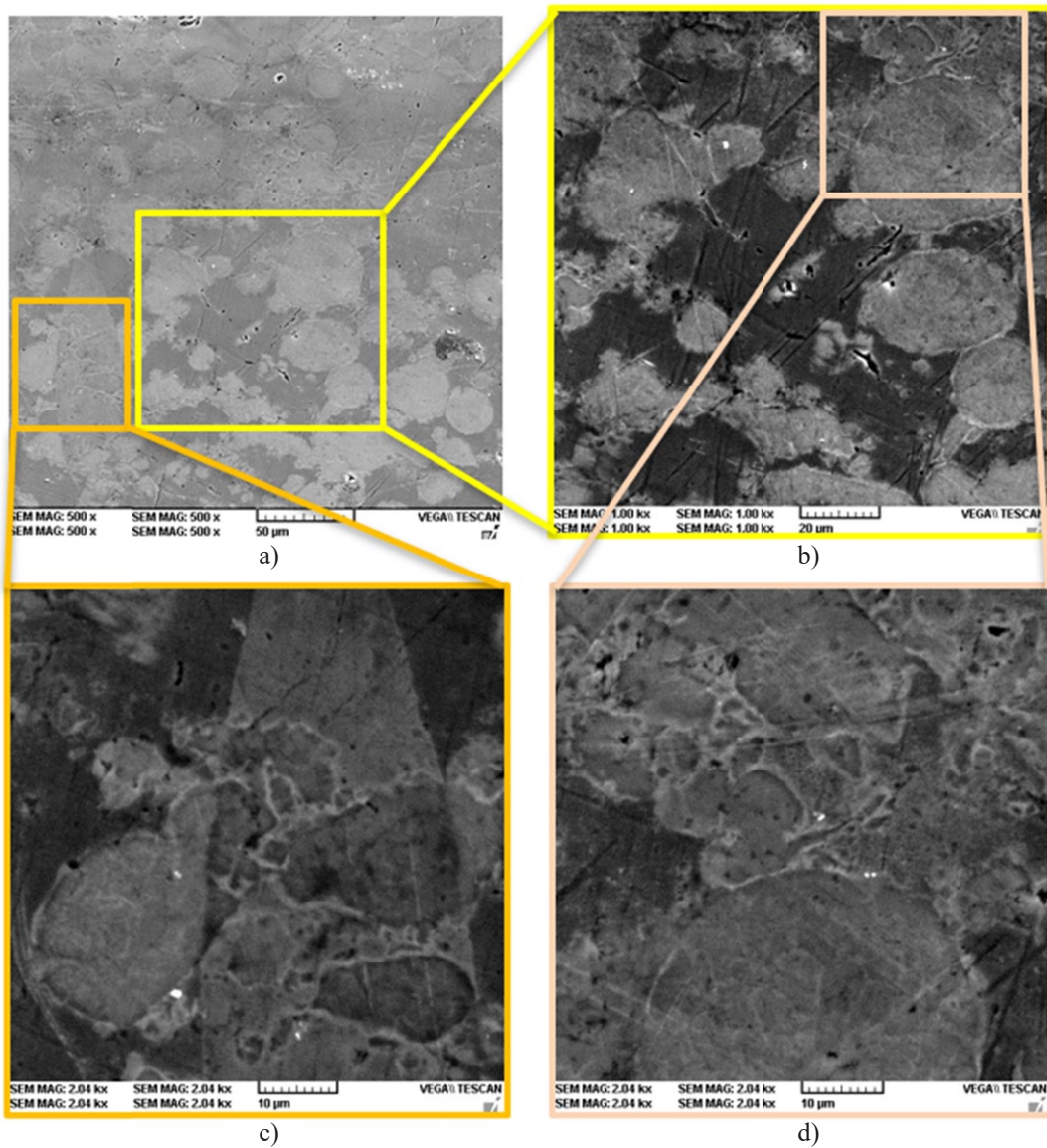
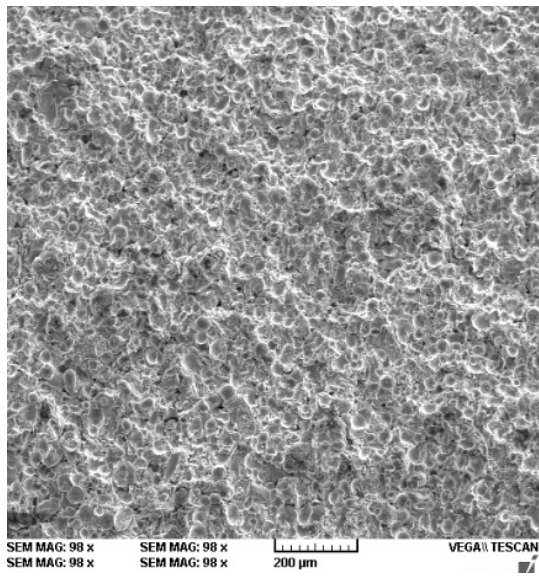
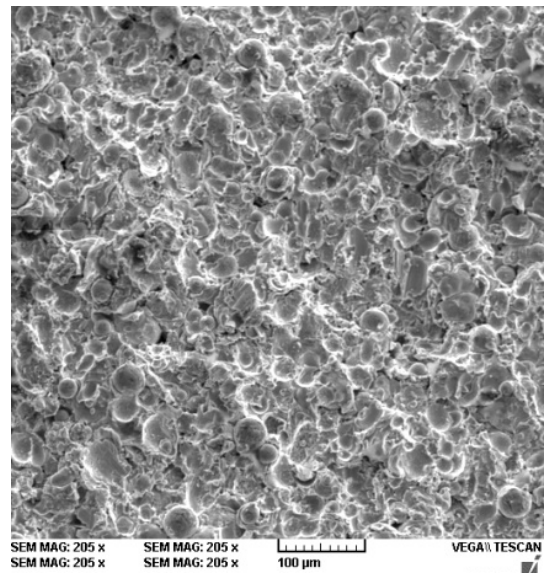


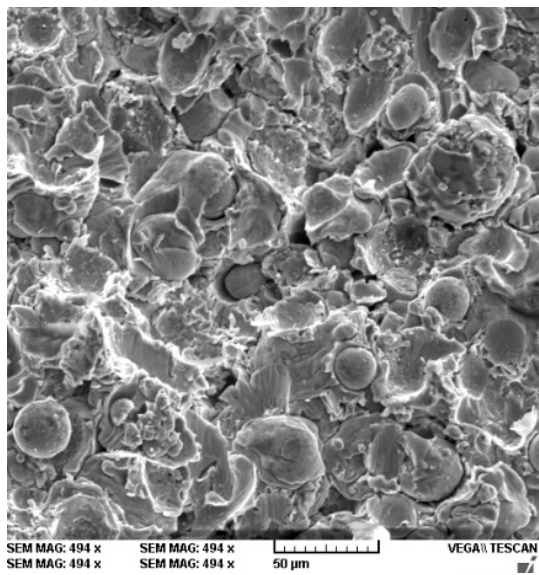
Fig. 8. Images of secondary electrons on the cross section of the coating: a) 500×, b) 1000×, c), d) 2000×



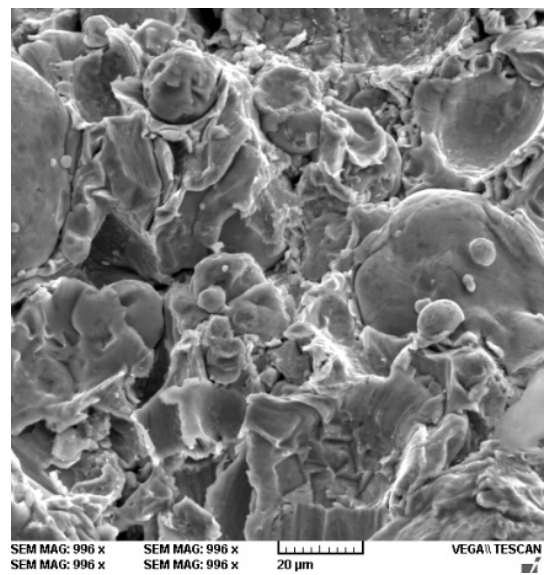
a)



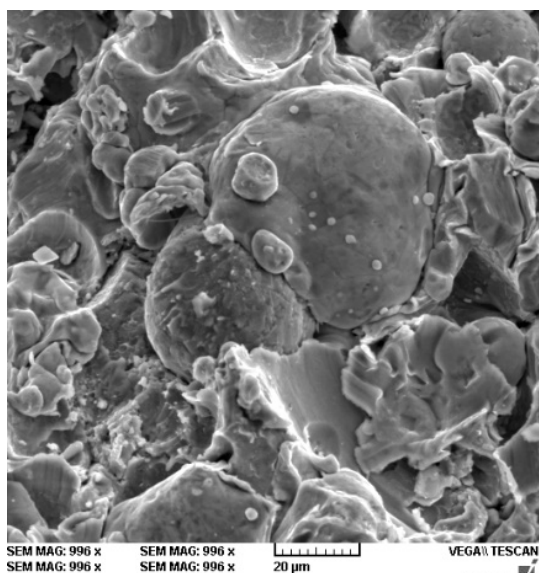
b)



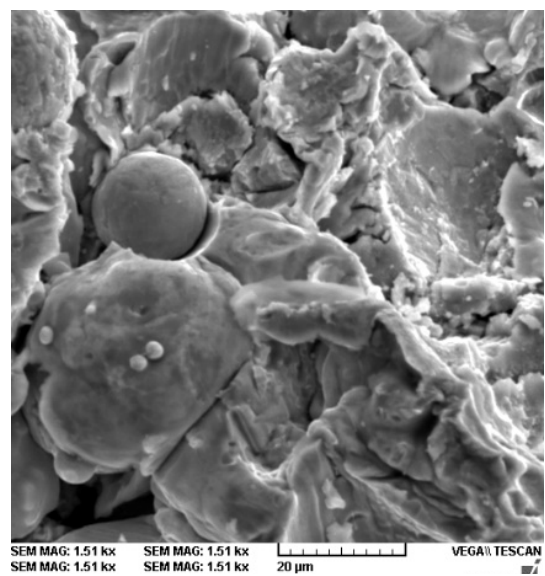
c)



d)



e)



f)

Fig. 9. Images of secondary electrons on the coating surface: (a) 100×, (b) 200×, (c) 500×, (d) 1000×, (e) 2000×

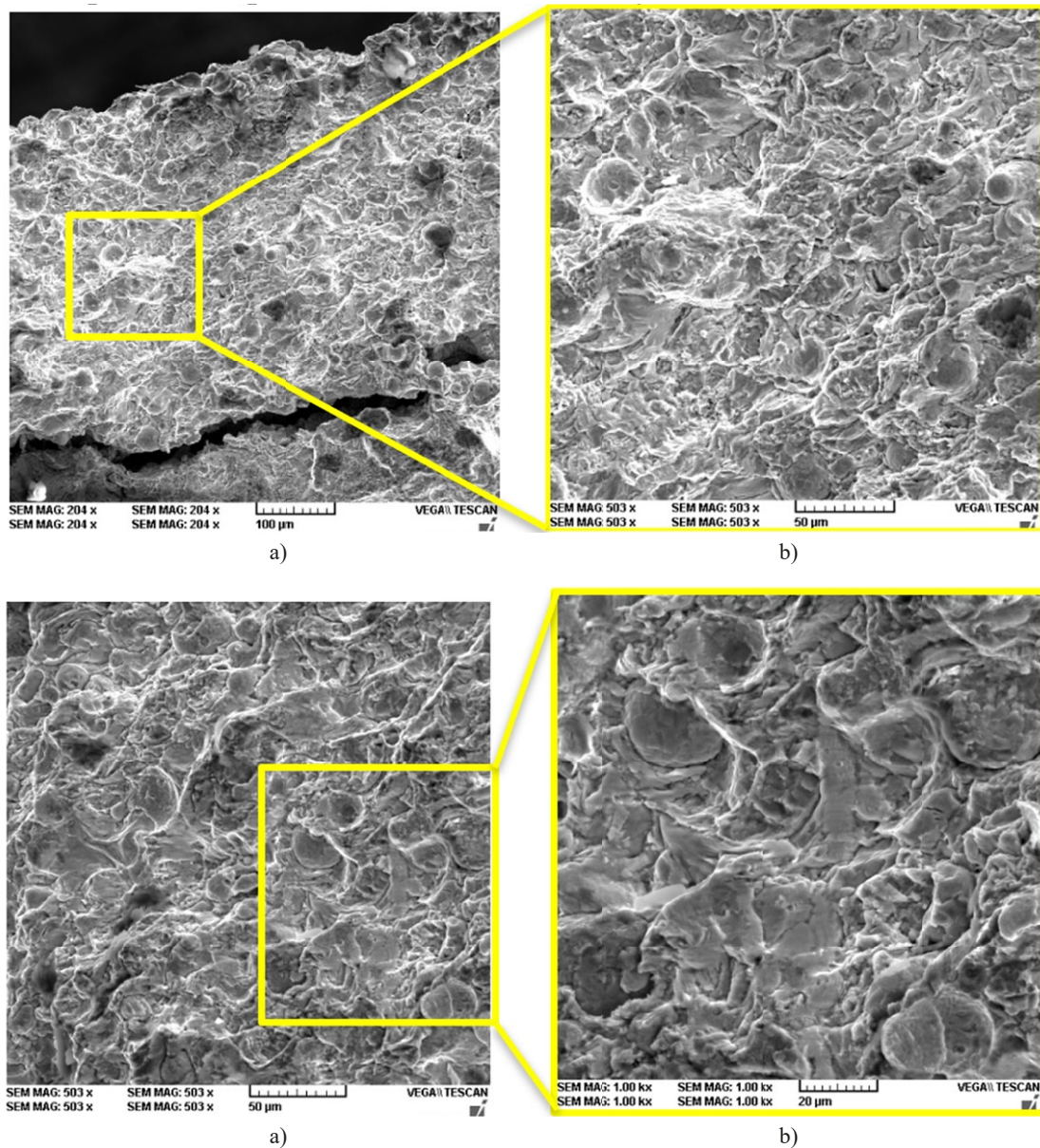


Fig. 10. Images of secondary electrons on the coating case: a), b) 200 \times , c), d) 500 \times

3.2. Chemical elements analysis

The elemental chemical analysis and the distribution map of the component elements shown in Fig. 11 show that the CrC particles have largely retained their sphericity, being uniformly embedded in the Ni matrix obtained from the plastic deformation of powders of this composition.

Another advantage of this type of deposition, shown on the chemical element distribution map, is the very low oxidation of the powdered particles, which brings with it a much better resistance of the whole layer.

The chemical distribution map on the coating surface (Fig. 12) shows, similarly to the cross-section map, a uniform distribution of the elements, i.e. the pulverized particles that formed the coating. The resulting mass values, presented in the table attached to Fig. 12, show a higher percentage of Ni element compared to the cross-section analysis, a plausible result because

chromium carbide (CrC) particles being mostly spherical are not stable unless fixed in the Ni matrix.

The distribution map shows, as in the two previous cases, a uniform presence of chemical elements, i.e. of powdered particles, the mass percentage of Ni being intermediate (59.2 wt.% in section <65.6 wt.% in fracture <70.7 wt.% on the surface).

4. Conclusions

Cold spray technology is an emerging technology that is not intended to replace any of the well-known thermal spray methods. Instead, it is intended to complement and extend the range of applications for thermal spraying processes as a greener alternative, in compliance with strict environmental and health safety regulations.

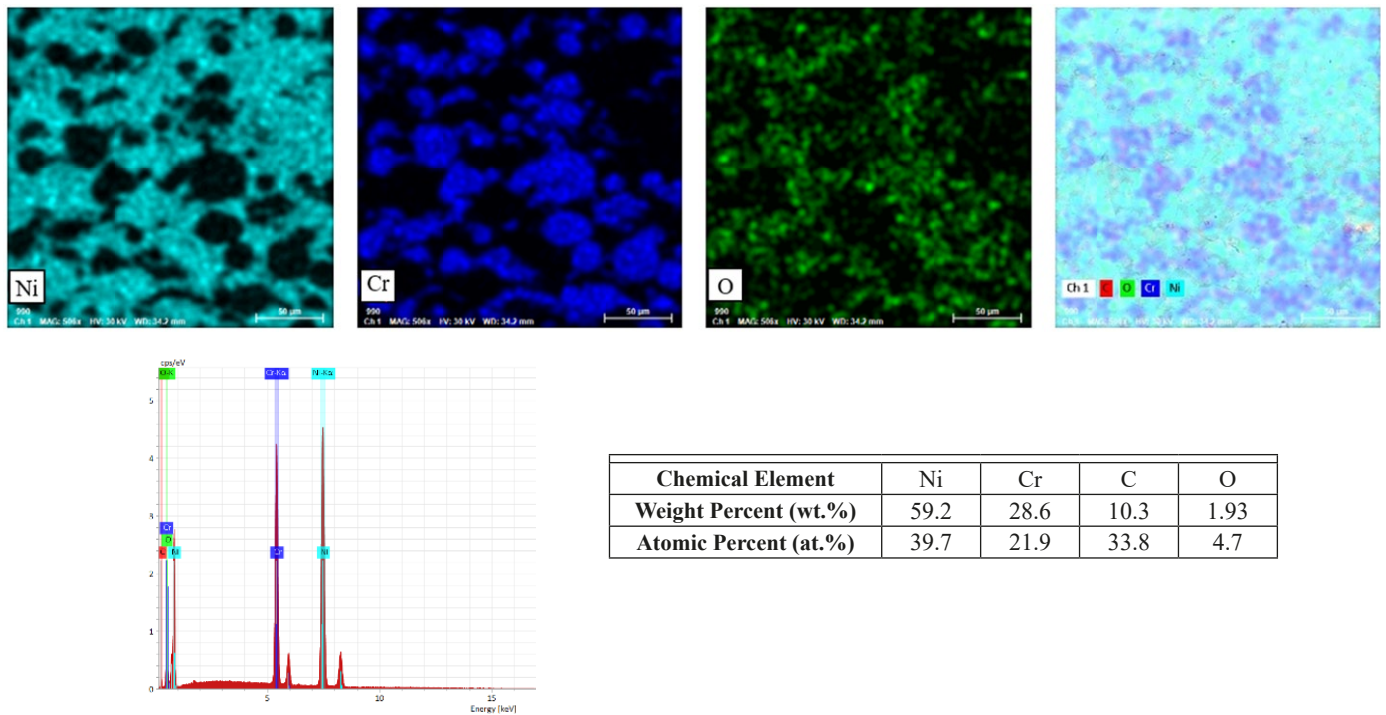


Fig. 11. Distribution map of chemical elements on the coating section in Fig. 8a and the resulting chemical composition

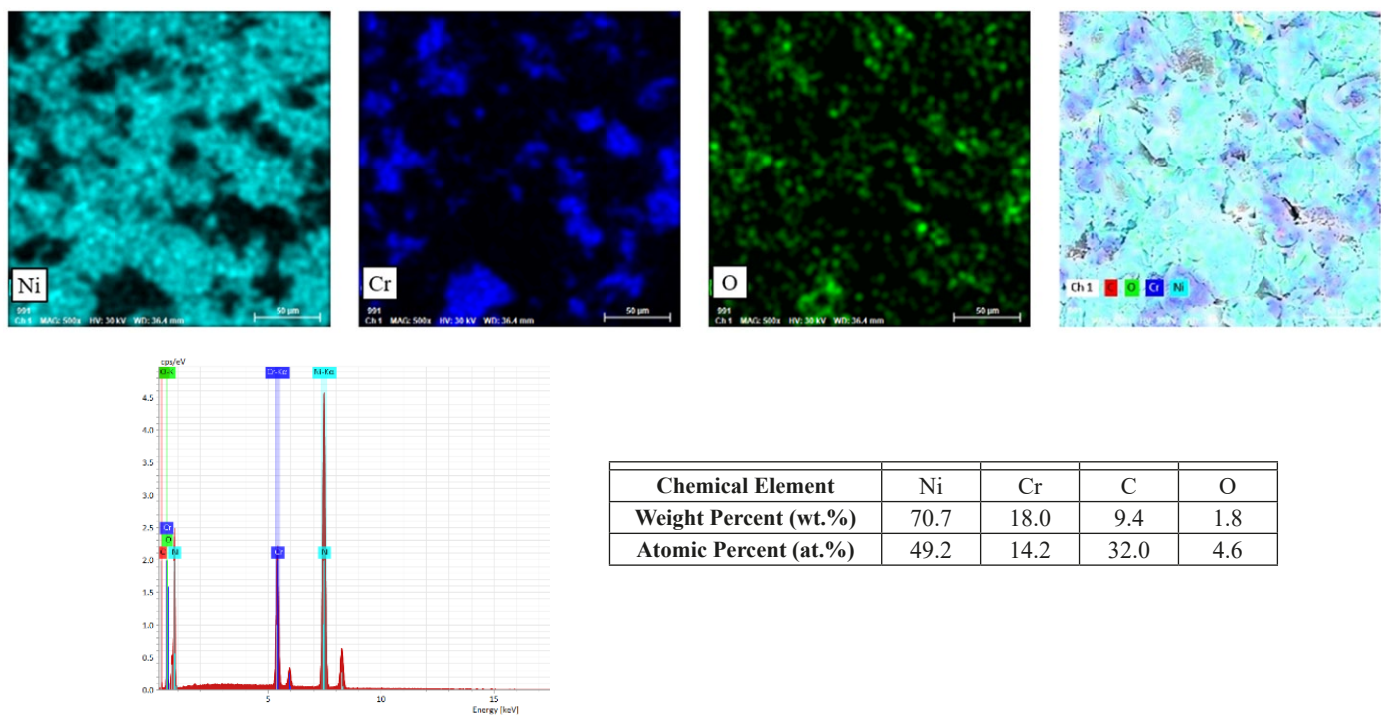


Fig. 12. Distribution map of chemical elements on the coating section in Fig. 9c and the resulting chemical composition

A range of materials has already proven suitable for cold spray deposition, from decorative items to biomedical, automotive, power plant and space industries. Extensive research is needed to design optimal parameters such as the nature of the gas, temperature control, nozzle design and nozzle material, and to predict the critical velocity for different particle/substrate combinations.

In the studied case, no adhesion defects were observed at the coating-deposited layer interface, the layer appearance is continuous, uniform and sinuous, characteristic for Cold Spray coatings. It was also observed that the steel substrate has also locally undergone major plastic deformation over a depth of a maximum 20 μm at the contact with the deposited layer, as a result of the supersonic impact with the solid sprayed particles during the coating process.

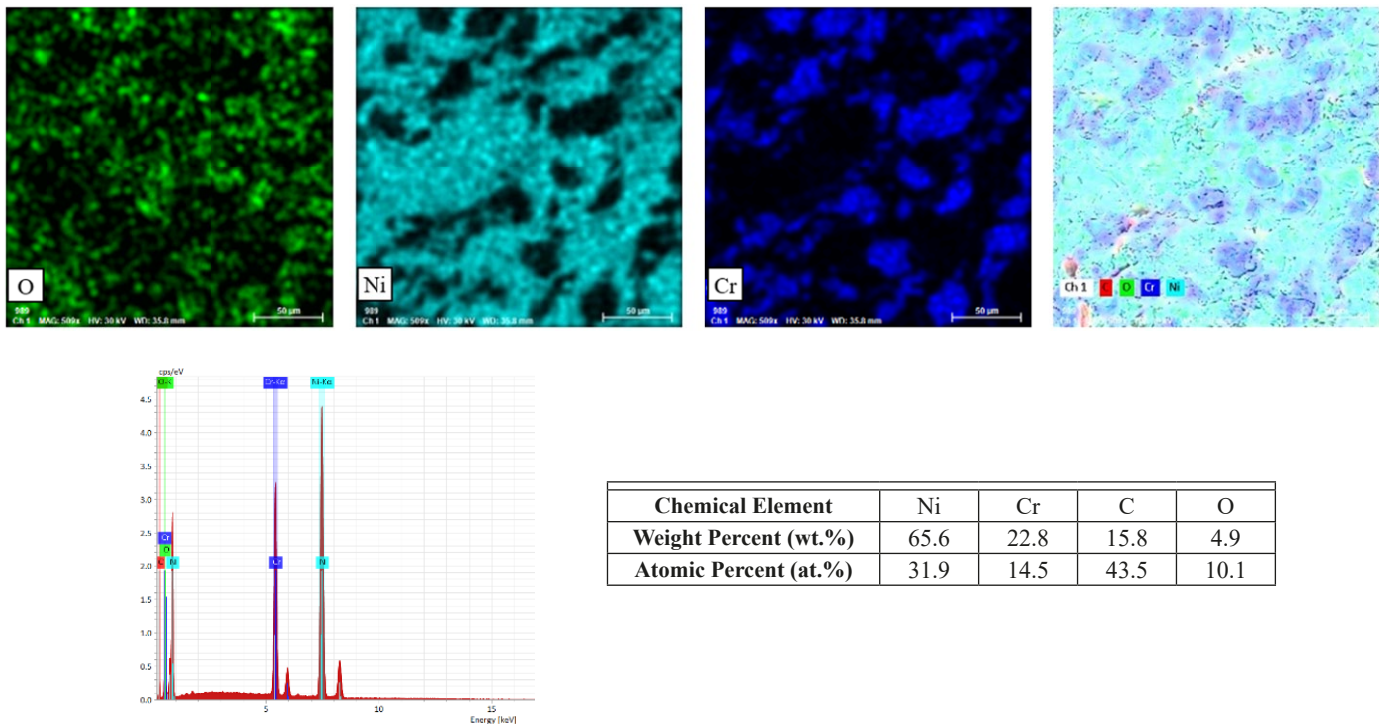


Fig. 13. Distribution map of chemical elements on the coating section in Fig. 10c and the resulting chemical composition

The elemental chemical analysis on the sample cross-section, together with the distribution map shows that the CrC particles have retained their sphericity to a large extent, being uniformly embedded in the Ni matrix, as a result of the plastic deformation.

Another advantage of this type of deposition, shown on the chemical element distribution map, is the very low oxidation of the powdered particles, which ensures a much better resistance of the whole layer.

Regarding the chemical element distribution maps, a uniform presence of chemical elements, i.e. pulverized particles, is observed in all three cases of analysis, the mass percentage of Ni being: 59.16 wt.% in cross-section <65.57 wt.% in fracture <70.71 wt.% on the surface.

The cold spray deposition technique is gradually gaining its place among the preferred methods of surface deposition of a diverse range of temperature-sensitive materials, such as those with high oxygen affinity (aluminium, copper and titanium) and those that undergo undesirable phase transformations at high temperatures, such as carbide-based composites. The coatings thus obtained can have considerable thicknesses of the order of millimetres without affecting the microstructure and without the danger of adhesion failure, due to the formation of a high-density structure.

REFERENCES

- [1] P. Poza, M.A. Garrido-Maneiro, Cold-sprayed coatings: Microstructure, mechanical properties, and wear behaviour. *Progress in Materials Science* **123**, 100839 (2022).
- [2] A. Papyrin, Cold spray technology. *Advanced Materials and Processes* **159** (9), 49-51(2001).
- [3] A.P. Alkhimov, A.N. Papyrin, V.F. Kosarev, N.I. Nesterovich, M.M. Shushpanov, Gas-dynamic spraying method for applying a coating (US 5302414): Patent; 1994.
- [4] H. Singh et al., Cold spray technology: future of coating deposition processes, *Frattura ed Integrità Strutturale* **22**, 69-84 (2012). DOI: <https://doi.org/10.3221/IGF-ESIS.22.08>
- [5] H. Assadi, H. Kreye, F. Gärtner, T. Klassen, Cold Spraying a materials perspective. Helmut Schmidt University, Institute of Materials Engineering, Hamburg, Germany.
- [6] E. Irissou, J. Legoux, A.N. Ryabinin, B. Jodoin, C. Moreau, Review on cold spray process and technology: Part I – Intellectual property. *Journal of Thermal Spray Technology* **17**, 495-516 (2008).
- [7] R.C. McCune, A.N. Papyrin, J.N. Hall, W.L. Riggs, P.H. Zajchowski, An exploration of the cold gas-dynamic spray method for several material systems. In: Berndt C.C., Sampath S. (Eds.). *Advances in Thermal Spray Science and Technology*. Materials Park: ASM International. p. 1-5 (1995).
- [8] R.C. Dykhuizen, M.F. Smith, Gas dynamic principles of cold spray. *Journal of Thermal Spray Technology* **7**, 205-212 (1998).
- [9] C.-J. Li, W.-Y. Li, Y.-Y. Wang, G.-J. Yang, H. Fukunuma, *Thin Solid Films*, 489 (2005) 79.
- [10] Q. Wang, M. Zhang, Review on recent research and development of cold spray technologies. *Key Engineering Materials* **533**, 1-52 (2013).
- [11] H. Kreye, T. Stoltenhoff, Cold spraying – a study of process and coating characteristics. In: *Proceedings of the International Thermal Spray Conference* 419-422 (2000). DOI: <https://doi.org/10.31399/asm.cp.itsc2000p0419>

- [12] V.F. Kosarev, S.V. Klinkov, A.P. Alkhimov, A.N. Papyrin, On some aspects of gas dynamics of the cold spray process. *Journal of Thermal Spray Technology* **122**, 65-281 (2003).
- [13] F. Gärtner, T. Schmidt, T. Stoltenhoff, H. Kreye, Recent developments and potential applications of cold spraying. *Advanced Engineering Materials* **8**, 611-618 (2006).
- [14] A. Moridi, S.M. Hassani-Gangaraj, M. Guagliano, M. Dao, Cold spray coating: Review of material systems and future perspectives. *Surface Engineering* **30**, 369-395(2014).
- [15] S. Grigoriev, A. Okunkova, A. Sova, P. Bertrand, I. Smurov, Cold spraying: From process fundamentals towards advanced applications. *Surface and Coatings Technology* **268**, 77-84. (2015).
- [16] T. Goyal, T.S. Sidhu, R.S. Walia, In: National Conference on Advancements and Futuristic Trends in Mechanical and Materials Engineering, 364 (2010).
- [17] J. Villafurerte, Current and Future Applications of Cold Spray Technology. *Metal Finishing* **108**, 1, 37-39 (2010). DOI: [https://doi.org/10.1016/S0026-0576\(10\)80005-4](https://doi.org/10.1016/S0026-0576(10)80005-4)
- [18] V. Goanta, C. Munteanu, S. Müftü, B. Istrate, P. Schwartz, S. Boese, G. Ferguson, C.I. Moraras, A. Stefan, Evaluation of the Fatigue Behavior and Failure Mechanisms of 4340 Steel Coated with WIP-C1 (Ni/CrC) by Cold Spray. *Materials* **15**, 8116 (2022). DOI: <https://doi.org/10.3390/ma15228116>
- [19] V. Goanta, C. Munteanu, S. Müftü, B. Istrate, P. Schwartz, S. Boese, G. Ferguson, C.I. Moraras, Evaluation of the Fatigue Behaviour and Failure Mechanisms of 52100 Steel Coated with WIP-C1 (Ni/CrC) by Cold Spray. *Materials* **15**, 3609 (2022). DOI: <https://doi.org/10.3390/ma15103609>
- [20] M. Pañțuru, D.L. Chicet, C. Munteanu, B. Istrate, P. Avram, Microstructural aspects at coating-substrate interface for some thermal sprayed layers on valve discs. *IOP Conf. Series: Materials Science and Engineering* **444**, 032009 (2018). DOI: <https://doi.org/10.1088/1757-899X/444/3/032009>